

NO-A176 194

COMPRESSIVE PROPERTIES AND LASER ABSORPTIVITY OF
UNIDIRECTIONAL METAL MAT. (U) AEROSPACE CORP EL SEGUNDO
CA LAB OPERATIONS D L CHANG ET AL. 30 SEP 86

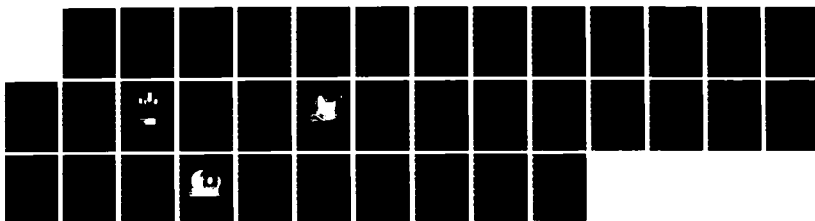
1/1

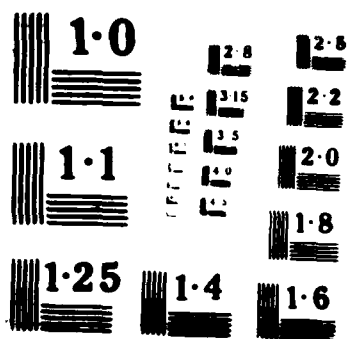
UNCLASSIFIED

TR-0084A(5935-14)-3 SD-TR-86-81

F/G 11/4

NL





121

Compressive Properties and Laser Absorptivity of Unidirectional Metal Matrix Composites

D. T. CHANG, G. E. SIECKEL, W. D. HANNA,
and E. IZAGUIRRE
Materials Sciences Laboratory
Laboratory Operations
The Aerospace Corporation
El Segundo, CA 90245

30 September 1986

Prepared for
SPACE DIVISION
AIR FORCE SYSTEMS COMMAND
Los Angeles Air Force Station
P.O. Box 92960, Worldway Postal Center
Los Angeles, CA 90009-2960

APPROVED FOR PUBLIC RELEASE
DISTRIBUTION UNLIMITED

AD-A176 194

AD-A176 194

121

This report was submitted by The Aerospace Corporation, El Segundo, CA 90245, under Contract No. F04701-85-C-0086 with the Space Division, P.O. Box 92960, Worldway Postal Center, Los Angeles, CA 90009-2960. It was reviewed and approved for The Aerospace Corporation by R. W. Fillers, Director, Materials Sciences Laboratory.

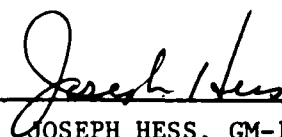
Lt. Donald Thoma, SD/YXTI, was the project officer for the Mission-Oriented Investigation and Experimentation (MOIE) Program.

This report has been reviewed by the Public Affairs Office (PAS) and is releasable to the National Technical Information Service (NTIS). At NTIS, it will be available to the general public, including foreign nationals.

This technical report has been reviewed and is approved for publication. Publication of this report does not constitute Air Force approval of the report's findings or conclusions. It is published only for the exchange and stimulation of ideas.



DONALD THOMA, Lt, USAF
MOIE Project Officer
SD/YXTI



JOSEPH HESS, GM-15
Director, AFSTC West Coast Office
AFSTC/WCO OL-AB

UNCLASSIFIED

SECURITY CLASSIFICATION OF THIS PAGE (When Data Entered)

REPORT DOCUMENTATION PAGE		READ INSTRUCTIONS BEFORE COMPLETING FORM
1. REPORT NUMBER SD-TR-86-81	2. GOVT ACCESSION NO. AD-A176194	3. RECIPIENT'S CATALOG NUMBER
4. TITLE (and Subtitle) Compressive Properties and Laser Absorptivity of Unidirectional Metal Matrix Composites		5. TYPE OF REPORT & PERIOD COVERED
7. AUTHOR(s) D. J. Chang, G. L. Steckel, W. D. Hanna, F. Izaguirre		6. PERFORMING ORG. REPORT NUMBER TR-0084A(5935-14)-3
9. PERFORMING ORGANIZATION NAME AND ADDRESS The Aerospace Corp. El Segundo, CA 90245		8. CONTRACT OR GRANT NUMBER(s) F04701-85-C-0086
11. CONTROLLING OFFICE NAME AND ADDRESS Space Division Los Angeles Air Force Station Los Angeles, CA 90009		10. PROGRAM ELEMENT, PROJECT, TASK AREA & WORK UNIT NUMBERS
14. MONITORING AGENCY NAME & ADDRESS (if different from Controlling Office)		12. REPORT DATE 30 September 1986
		13. NUMBER OF PAGES 30
		15. SECURITY CLASS. (of this report) Unclassified
		15a. DECLASSIFICATION/DOWNGRADING SCHEDULE
16. DISTRIBUTION STATEMENT (of this Report) Approved for public release; distribution unlimited.		
17. DISTRIBUTION STATEMENT (of the abstract entered in Block 20, if different from Report)		
18. SUPPLEMENTARY NOTES		
19. KEY WORDS (Continue on reverse side if necessary and identify by block number) Metal matrix composite Laser absorptivity Compressive properties		
20. ABSTRACT (Continue on reverse side if necessary and identify by block number) MMC use has been impeded because there is no well qualified property data base. Elevated temperature compressive properties and laser absorptivity data are in great demand in the design, modelling, and analysis of MMC structures in elevated temperature applications and survivability assessment. Testing methods were developed for room temperature and elevated temperature compressive modulus and strength measurements of single-ply unidirectional graphite-aluminum (Gr/Al) and graphite-magnesium (Gr/Mg), and to generate laser absorptivity data for these two types of materials.		

DD FORM 1473
(FACSIMILE)

UNCLASSIFIED

SECURITY CLASSIFICATION OF THIS PAGE (When Data Entered)

UNCLASSIFIED

SECURITY CLASSIFICATION OF THIS PAGE(When Data Entered)

19. KEY WORDS (Continued)

20. ABSTRACT (Continued)

→ An effective gage length was established for valid compression tests to eliminate buckling failure. The measured failure strength values for Gr/Al and Gr/Mg are approximately 50 to 60% lower than the material tensile strength. Small gage strain gages are being used to measure the compressive modulus as a function of temperature.

The laser absorptivities of Gr/Al and Gr/Mg were measured by the use of an in-house developed differential calorimeter. The calorimeter has been used to measure total hemispherical emittance and normal laser absorptance of specimens as a function of temperature from 200 to 700°C.

Test results indicated that the laser absorptances of Gr/Al and Gr/Mg at 10.6 μm wavelength remain more or less constant over most of the temperature range tested.

micrometer

UNCLASSIFIED

SECURITY CLASSIFICATION OF THIS PAGE(When Data Entered)

CONTENTS

I.	INTRODUCTION.....	7
II.	PROCEDURE.....	9
III.	EXPERIMENTAL WORK.....	13
	A. Compression Tests.....	13
	B. Absorptance and Emittance Tests.....	16
IV.	RESULTS.....	25
	A. Compressive Tests.....	25
	B. Absorptance and Emittance Tests.....	29
V.	CONCLUSIONS AND RECOMMENDATIONS.....	33
	REFERENCES.....	35



[Faint, illegible handwritten notes]

[Handwritten mark resembling a stylized 'A' or '7' inside a box]

[Faint, illegible handwritten notes]

[Large handwritten number '11' at the bottom left]

FIGURES

1.	Compressive test fixture with conical wedges.....	14
2.	Photograph of compressive test fixture.....	15
3.	Schematic diagram of calorimeter.....	17
4.	Photograph of calorimeter.....	18
5.	Laser beam path.....	20
6.	Expected behavior of power controllers' output.....	21
7.	Absorptance of 6061-T6 aluminum, graphite-aluminum, and graphite-magnesium as a function of temperature.....	30
8.	Calorimeter disassembled after absorptance tests.....	31
9.	Total hemispherical emittance of 6061 aluminum, graphite-aluminum, and graphite-magnesium as a function of temperature.....	32

TABLES

1.	Panel Composition and Configuration of Unidirectional Gr/Al and Gr/Mg Materials.....	10
2.	Compressive Moduli of Unidirectional Gr/Al and Gr/Mg.....	26
3.	Compressive Strength of Unidirectional Gr/Al and Gr/Mg.....	27

1. INTRODUCTION

The development of metal matrix composite (MMC) materials was initiated in the early 1950's. The goal of the development work was to fabricate composite materials that offer characteristics such as high strength and modulus, light weight, and high temperature load carrying capability. Early work included the investigation of boron aluminum, boron titanium, silicon carbide aluminum, silicon carbide titanium, and alumina (DuPont FP) reinforced composites [1-2]. Significant data have been presented over the past decades, especially for boron aluminum composites [3-13] because of the high modulus and strength and low density of boron fibers.

Graphite fiber reinforced composites have been shown to have lower density, which is a very important selection parameter for space applications. Furthermore, graphite fibers generally have a negative coefficient of thermal expansion (CTE) over the temperature range of specific interest. Much work has been done to demonstrate that graphite fiber reinforced composite materials can be fabricated with nearly zero thermal dimensional growth [14,15]. Thus, it provides great dimensional stability to fulfill stringent distortional requirements. The dimensional stability provided by graphite fiber reinforced composite is unique and cannot be achieved by other known MMC materials.

Recent development of graphite fibers has resulted in higher stiffness fibers (P100, P120, and P140) with 6.89 to 9.65×10^5 MN/m² (100 to 140 Msi) moduli. Unidirectionally reinforced MMC fabricated from these types of fibers offers greater axial stiffness for structure components such as struts, booms, and tower structures. Thin ply fabricability and the feasibility of producing complex shapes have been demonstrated for graphite-aluminum (Gr/Al) and graphite-magnesium (Gr/Mg). Mechanical properties such as tensile moduli and strengths, and thermal physical properties have been measured for these materials by various investigators [15-17].

However, other basic properties such as compressive moduli and strengths, shear moduli and strengths, fracture behavior, optical absorptance and

emittance for these materials are at best very limited in the literature. Data to evaluate these properties for the design, analysis, and modelling of MMC are useful to permit development of structural components for room and high temperature applications. The utilization of the potential of MMC will be severely hindered unless these properties become available. Work has been performed at The Aerospace Corporation to develop the testing methodology and to generate data for some of the basic properties. These investigations have included the compressive properties and laser absorptance for Gr/Al and Gr/Mg materials as a function of temperature. The results of the work will assist the establishment of standard testing techniques, and the broadening of the data base for design, modelling and analysis, and failure criteria.

II. PROCEDURE

Two types of MMC were utilized in the project: 6061 graphite aluminum and AZ91C graphite magnesium with AZ61A surface foils. The graphite fibers were P100 (VS-0054) mesophase pitch fibers with an average axial direction modulus of elasticity of $7.24 \times 10^5 \text{ MN/m}^2$ ($105 \times 10^6 \text{ psi}$) and an average density and ultimate strength of 2.15 g/cm^3 (0.078 lb/in^3) and 2.24 MN/m^2 ($325 \times 10^3 \text{ psi}$), respectively. The fibers were manufactured by Union Carbide Corp. and the 6061 Gr/Al and AZ91C Gr/Mg wires were made by Materials Concepts, Inc. (MCI), Columbus, Ohio. Two types of specimens were fabricated. Unidirectional single layer Gr/Al and Gr/Mg plates were fabricated by DWA Composite Specialties, Inc., Chatsworth, CA., with 0.089 mm (3.5 mil) thick 6061 aluminum and 0.076 mm (3.0 mil) thick AZ61A magnesium surface foils, respectively. The compressive specimens were machined from these plates. Their nominal dimensions are 11.43 cm long \times 0.64 cm wide (4.5 in. long \times 0.25 in. wide). The use of single ply specimen was dictated by the lightweight requirement in actual applications. For the laser absorptance tests, thicker specimens were fabricated because of the design requirements of the apparatus employed. The panels were diffusion bonded by DWA by stacking up ten single-layer unidirectional layups. The fabrication parameters include: 588°C (1090°F) at 24 MN/m^2 ($3.5 \times 10^3 \text{ psi}$) for 20 min. for Gr/Al; 477°C (890°F) at 24 MN/m^2 ($3.5 \times 10^3 \text{ psi}$) for 40 min. for Gr/Mg. Table 1 shows the fiber, matrix, and fiber volume of the fabricated panels. Since the thick panels had the same diffusion bonding parameters, it is expected that they had surface conditions similar to those of the single layer panels.

Thermo-optical properties of engineering materials are generally not available. This is particularly true for properties at elevated temperatures. Furthermore, such properties are affected by handling and other environmental or processing conditions to such an extent that direct measurements taken on specific materials of interest are often the only means of obtaining data with which one can confidently model material response to thermal radiation inputs. Total hemispherical emittance and directional laser absorptance of MMC materials can vary considerably depending, among other things, on surface deformations due to the underlying matrix, thermal

TABLE 1. Panel Composition and Configuration of Unidirectional
Gr/Al and Gr/Mg Materials

Materials	Matrix	Surface Foil	Fiber Volume Fraction %	Specimen Thickness, mm(in.)	Remarks
Gr/Al	6061	0.089 mm (3.5 mil) 6061 Al	33.0	0.686 (.027)	For unidirectional compression tests
Gr/Mg	AZ91C	0.061 mm (2.4 mil) AZ61A	37.0	0.655 (0.026)	For unidirectional compression tests
Gr/Al	6061	0.089 mm (3.5 mil) 6061 Al	32.6	6.50 (0.256)	For emittance and laser absorptance tests
Gr/Mg	AZ91C	0.076 mm (3.0 mil) AZ61A	32.8	5.75 (0.226)	For emittance and laser absorptance tests

diffusivity through the normal axis of the matrix, and surface alloy composition.

III. EXPERIMENTAL WORK

A. COMPRESSION TESTS

All compression tests were performed with the use of a modified ASTM D3410 Celanese fixture. The fixture had a smaller overall diameter so that it could be fit in a quad-elliptical, high-intensity, infrared, radiant heating chamber for high-temperature testing. The fixture was fabricated from Inconel 625 alloy so that testing at temperatures over 500°C (~ 930°F) could be performed. Figure 1 is a sketch of the compressive test fixture and Fig. 2 is a photograph of the fabricated fixture.

The modified D3410 fixture was selected for the testing because it was found by Adsit [18] to give valid compression results. Although the pyramidal wedges [Illinois Institute of Technology Research Institute (IITRI) method] appear to give equivalent modulus and strength values for thin composite materials, such as graphite-epoxy, it may not have a symmetric temperature gradient when heated in an annular clamshell-type heater.

Tabs made from hard file material were used to transfer the shear load from the shell frustra to the specimens. Each of the four tabs was tapered at one end to produce uniform load transfer between the tabs and specimens. Moreover, the tabs acted as lateral supports to reduce possible transverse deflections which can cause the specimens to fail in a buckling rather than a compressive mode.

The compressive loads were applied using an Instron universal loading fixture, model 1135. Two Micro-Measurement Unidirectional EA-06-015-EH-120 strain gages were mounted at the center of the two surfaces of each specimen. The small strain gages, which have 0.015 in. gage length and 0.025 in. overall length, were chosen because a short unsupported specimen length was required to give valid compressive strengths, as will be discussed in the next section.

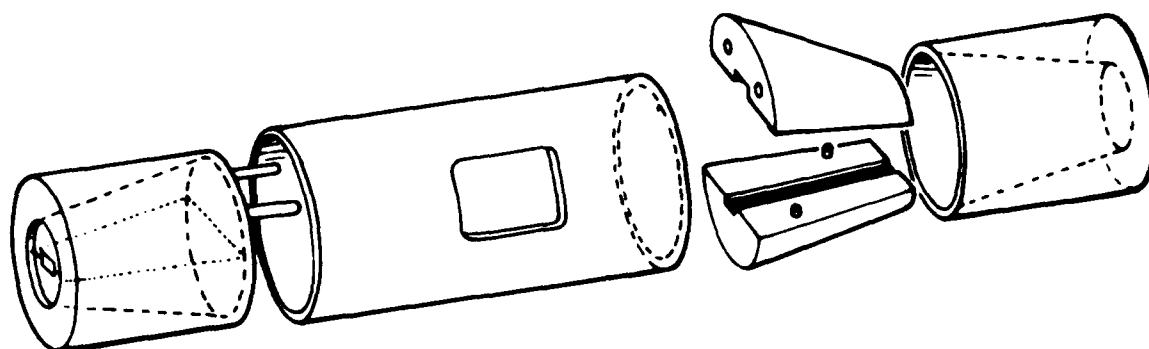
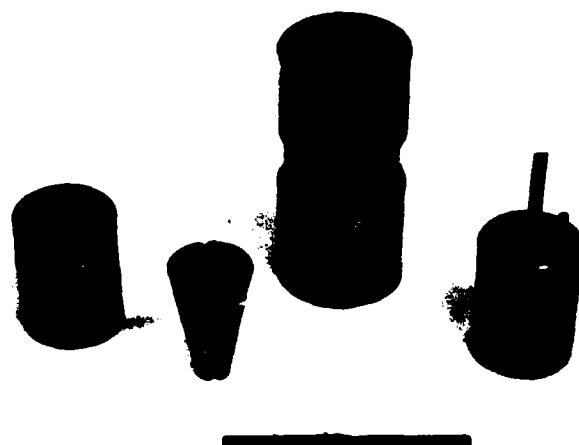


Fig. 1. Compressive test fixture with conical wedges



(a)



(b)

Fig. 2. Photograph of compressive test fixture (a) disassembled parts, (b) assembled fixture

B. ABSORPTANCE AND EMITTANCE TESTS

The normal spectral absorptance $\alpha_N(\lambda, T)$ and total hemispherical emittance $\epsilon(2\pi, T)$ testing of Gr/Al and Gr/Mg materials was performed as a function of temperature. The tests were carried out using an Aerospace-developed dual calorimeter [19]. The Gr/Al and Gr/Mg samples tested were disks 2 in. in diameter and approximately 1/4-in. (ten plies) thick. A control sample of 6061-T6 aluminum was also tested.

A schematic diagram of the calorimeter is shown in Fig. 3. The central part of the calorimeter is an oxygen-free, high-conductivity (OFHC) copper housing that provides a high-temperature environment for two sample assemblies. The housing consists of a main body and two end pieces. Each sample to be tested is mounted against an OFHC copper block in which two cartridge heaters are imbedded. The two sample assemblies are then positioned in the openings in both end pieces and are held in place by point contact with threaded stainless steel rods. The sample is mounted flush to the front surface of the end piece. An annular gap of about 0.025 in. separates the sample assembly from the end piece. The housing is heated separately from the dual sample assemblies by a clamshell-type heater. The assembled calorimeter is encased in a gold-coated stainless steel jacket. The temperatures of each sample and of the housing of the calorimeter are controlled independently. To allow the recording equipment to constantly monitor the power output, the temperature and power controllers are current proportional rather than time proportional. Power transducers continuously monitor the output of the power controllers and provide proportional voltage signals that are recorded. All electronic devices are hard-wired into a single console. To track the temperature of critical areas the assembly is instrumented with 20 thermocouples (see Fig. 4).

During the experiment, the assembled calorimeter is placed in a vacuum chamber. The interior of the chamber is surrounded with a cooling shroud. Calculations of the view factors [19] show that of all the surfaces seen by the sample, the largest view factor corresponds to the one between the sample and the shroud. To minimize the errors introduced by the uncertainty in the

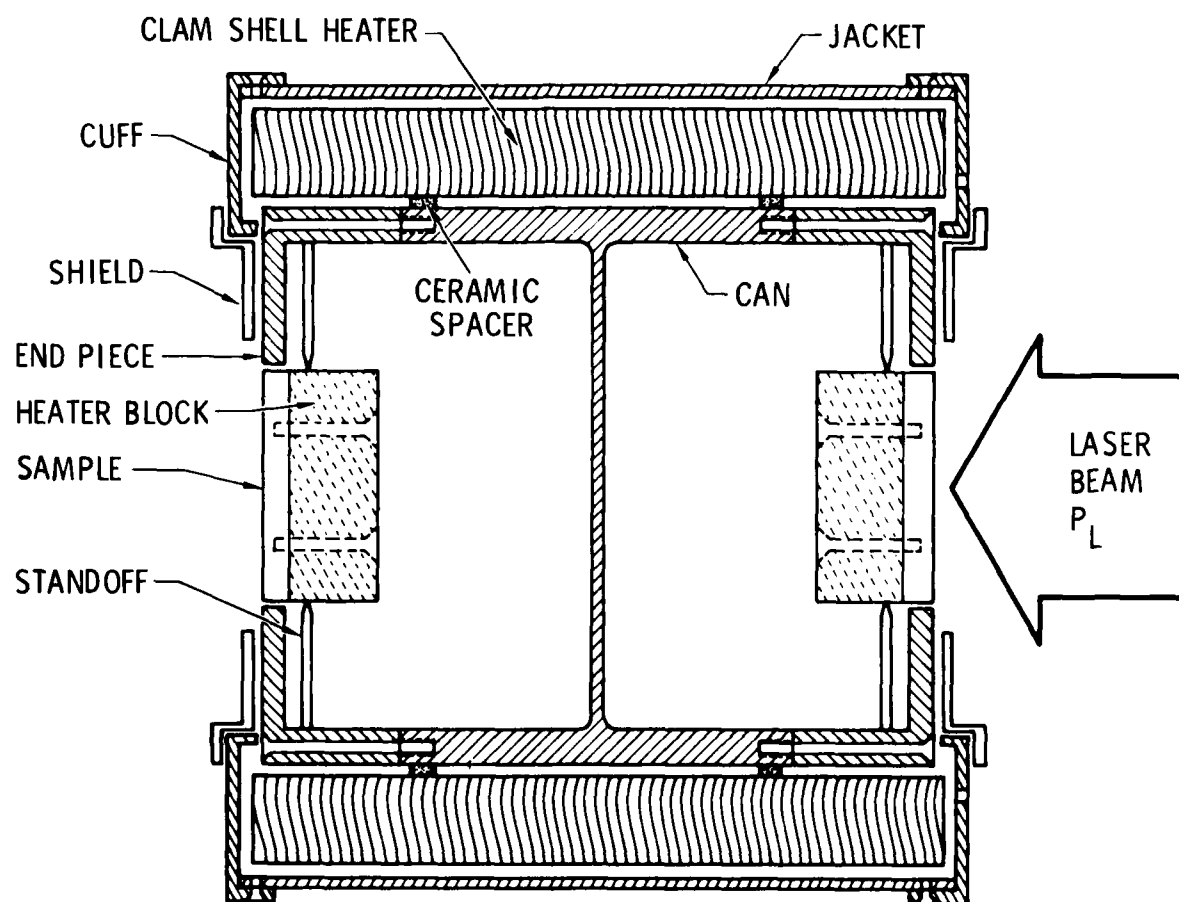


Fig. 3. Schematic diagram of calorimeter

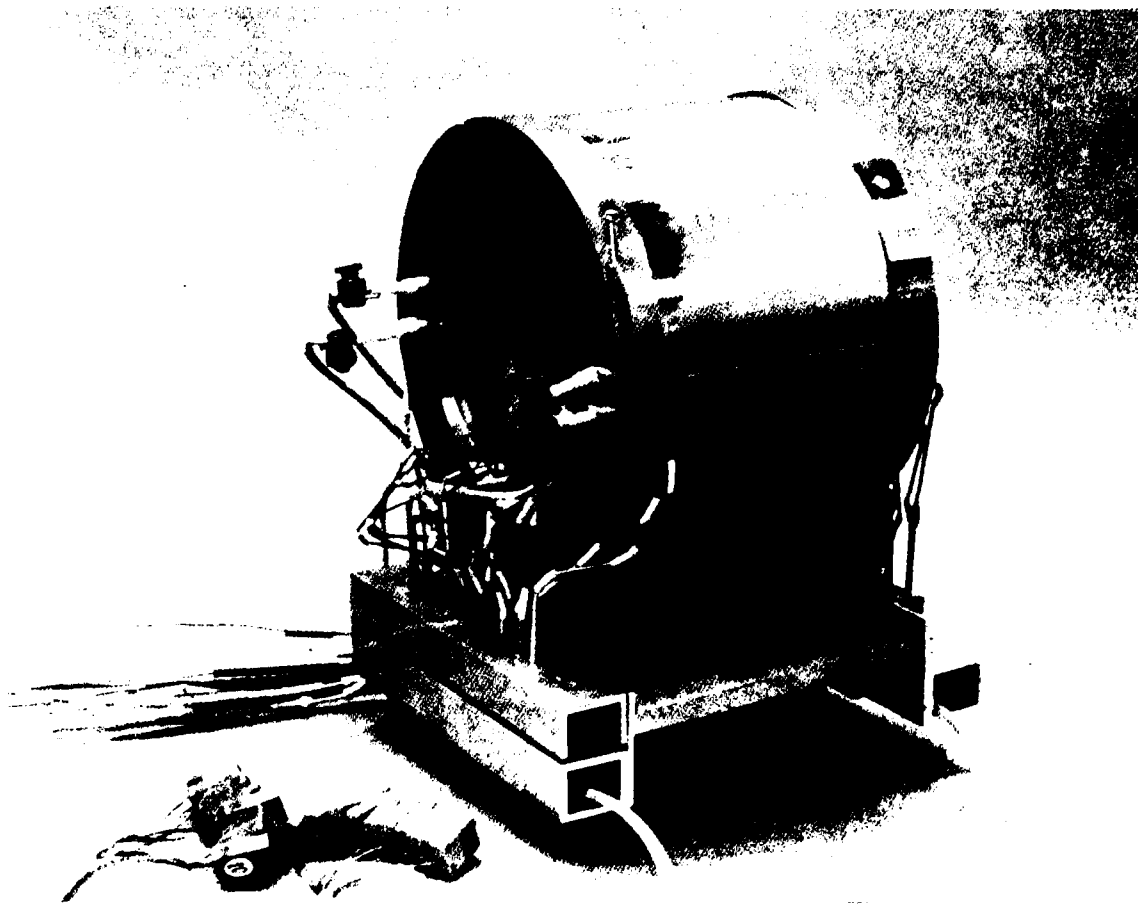


Fig. 4. Photograph of calorimeter

emittance of the shroud surface, the cooling passages in the shroud are filled with liquid nitrogen and its temperature is measured with thermocouples.

Figure 5 shows the CO₂ laser beam path. A sodium chloride wedge splits the beam. One reflection from the wedge is directed to a focussing mirror and into a power meter. The other reflection is steered toward the test chamber. The last mirror in this optical path focuses the beam onto the sample. The calorimeter is positioned and aligned in the vacuum chamber so that the beam is about the same size as the test sample and incident on the entire sample. The advantage of a dual calorimeter design is that it provides a convenient way of differentiating thermal damage from purely laser damage. If, when the absorptance is measured, the illuminated sample degrades while the other sample does not, then degradation is due to the absorptance of the sample at the particular wavelength of the laser being used.

The equation used to determine the normal spectral absorptance at a particular laser wavelength and a pre-determined temperature is

$$\alpha_N(\lambda, T) = \frac{P_2 - P_1}{P_L}$$

where

$\alpha_N(\lambda, T)$ = Normal absorptance as a function of wavelength and temperature

P_2 = Net electrical power delivered to the sample heating block before illumination of the sample with the laser

P_1 = Net electrical power delivered to the sample while the sample is being illuminated by the laser

P_L = Power delivered to the sample by the laser

The above equation assumes that all three powers, P_2 , P_1 , and P_L are measured at an equilibrium temperature and the temperature is the same before and after illumination of the sample by the laser. A graphic derivation of this equation can be deduced from Fig. 6.

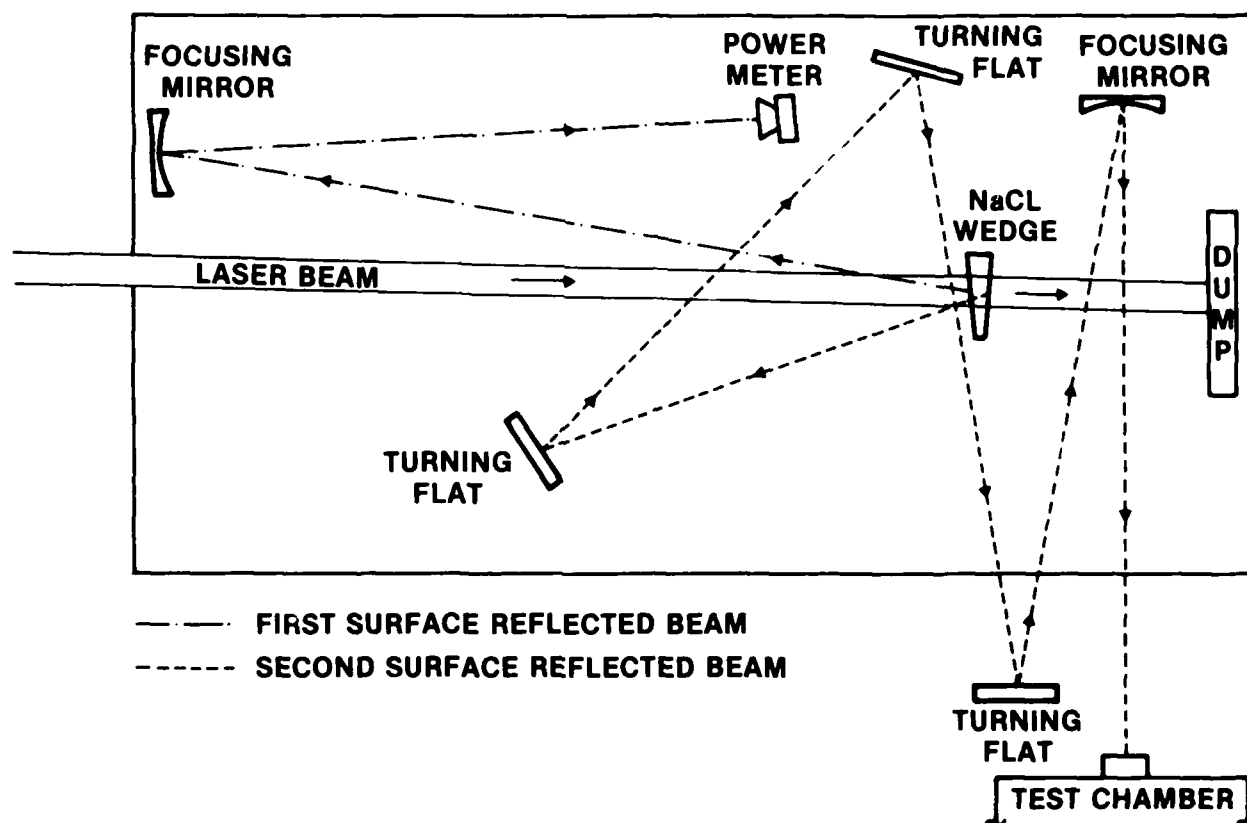


Fig. 5. Laser beam path

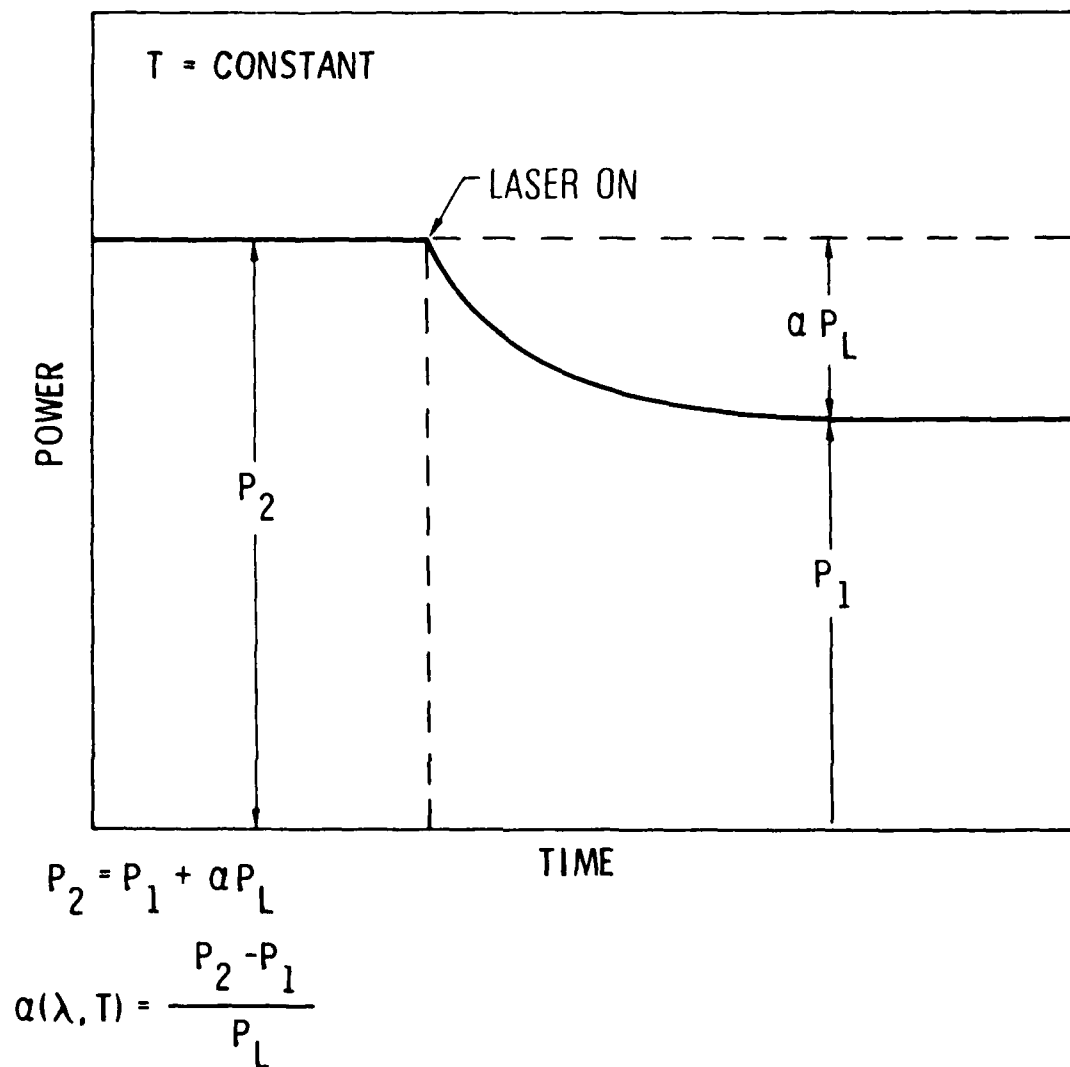


Fig. 6. Expected behavior of power controllers' output

The equation used to determine the total hemispherical emittance is

$$\epsilon(2\pi, T) = \frac{P_2}{A\sigma \sum_{i=2}^n F_{1,i} (T_1^4 - \epsilon_i T_i^4)}$$

where

$\epsilon(2\pi, T)$ = Total hemispherical emittance

P_2 = Net electrical power delivered to the sample heating block

A = Area of emitting surface

σ = Stefan-Boltzmann constant

$F_{1,i}$ = View factors between sample and surfaces seen by the sample

T_1 = Temperature of sample

T_i = Temperature of the surfaces seen by the sample

ϵ_i = Emittance of the surfaces seen by the sample

The major uncertainty in this equation is in ϵ_i . This uncertainty is negligible when $T_1 \gg T_i$. This condition can be attained by chilling the walls of the shroud as described above. For other surfaces, where it is not possible to lower the temperature, the view factors are small and the error remains negligible.

The preparation of the test samples included several steps. Blind mounting holes were drilled and tapped into the back of each sample and this surface was polished to ensure good thermal contact with the heating block. The surface to be tested for emittance and absorptance was cleaned with fine and very fine 3M Scotch Brite. Particular care was taken to avoid altering the surface roughness. Acetone was used to remove any residue from the cleaning process.

In addition to the two MMCs, a solid block of 6061-T6 Al was machined and used as a baseline sample. Its surface was cleaned in the same manner as the metal matrix samples. However, to eliminate machine oil, this sample was degreased in a hot bath of trichloroethane.

At the center of the back (nonexposed) surface of each sample, a small blind hole was drilled and a thermocouple inserted as near as possible to the front (exposed) surface. An additional thermocouple was sandwiched between the sample and the heating block. By means of these thermocouples the temperature gradient between the front and back surface of each sample during testing was observed to be no larger than 1°C . The test sample disks were anchored with screws to the heating blocks and then assembled in the calorimeter. The calorimeter was then placed in a vacuum chamber and the shroud of the chamber cooled with liquid nitrogen. The operational pressure was about 200 mT at the low end of the temperature scale, increasing to about 300 mT at the high end.

IV. RESULTS

A. COMPRESSIVE TESTS

Compressive tests were performed at 24, 149, and 260°C (75, 300, and 500°F) for compressive modulus and strength measurements. A 2.5 mm (0.1 in.) unsupported gage length between the tips of two tabs was used. This dimension was established after compression testing at several different gage lengths. It was found that failure occurred prematurely in buckling modes when the unsupported gage length was greater than 2.5 mm (0.1 in.) for single layer unidirectional Gr/Al and Gr/Mg composites. Table 2 summarizes the compressive modulus results, and Table 3 lists the results of the compressive strength. The room temperature tensile modulus and strength for specimens from the same panels as the compressive specimens were also tested and are shown in the two tables for comparison purposes. It can be seen from these two tables that the average room temperature compressive modulus for Gr/Al material is 2.12×10^5 MN/m² (30.7 Msi) which is about 78% of the room temperature tensile modulus, and the room temperature compressive strength is 272 MN/m² (39.4 ksi) which is about 36% of the room temperature tensile strength. The corresponding ratios for Gr/Mg material are 89% for room temperature modulus and 58.1% for the room temperature strength.

The compressive modulus of a single graphite fiber is almost impossible to measure since it is only $7 \sim 10 \mu\text{m}$ ($2.76 \sim 3.94 \times 10^{-4}$ in.) in diameter. It is believed to be similar to the tensile modulus. In general, the compressive modulus of a unidirectional graphite fiber reinforced composite is lower than the tensile modulus. The primary reason is that the graphite fibers can never be straight. There are kinks, bends, or even off-angle lay-ups which would make the compressive modulus lower even if the fiber tensile and compressive moduli were the same. In addition, the high processing temperature of Gr/Al and Gr/Mg puts the graphite fibers in compression as a result of cooling. This would either make the kinks and bends more pronounced or create new kinks and bends due to weak lateral support which would further lower the compressive modulus. Therefore, a compressive modulus of Gr/Al and Gr/Mg composites lower than the tensile modulus is expected.

TABLE 2. Compressive Moduli of Unidirectional Gr/Al and Gr/Mg

Material	Room Temperature Tensile Modulus, 10^5 MN/(Msi)	Temperature, °C (°F)	Compressive Modulus, 10^5 MN/m ² (Msi)
Gr/Al	2.71 (39.4)	24 (75)	2.12 (30.7)
		149 (300)	2.51 (36.4)
		260 (500)	2.71 (36.8)
Gr/Mg	2.90 (42.1)	24 (75)	2.58 (37.4)
		149 (300)	2.47 (35.9)
		260 (500)	2.63 (38.1)

TABLE 3. Compressive Strength of Unidirectional Gr/Al and Gr/Mg

Material	Room Temperature Tensile Strength, MN/m ² (ksi)	Temperature,		Compressive Strength, MN/m ² (ksi)
		°C	(°F)	
Gr/Al	751.4 (109)	24	(75)	271.6 (39.4)
		149	(300)	283.3 (41.1)
		260	(500)	228.9 (33.2)
Gr/Mg	488.8 (70.9)	24	(75)	284.0 (41.2)
		149	(300)	294.0 (42.2)
		260	(500)	213.7 (31.0)

No elevated tensile modulus and strength measurements were made on the same lots of materials that were used for compression tests. However, tensile tests were performed for 30% fiber volume fraction of Gr/Al and 45% fiber volume fraction of Gr/Mg fabricated by DWA using the same techniques. The data show a 9% tensile modulus decrease for RT to 260°C (500°F) and an 18% tensile strength variation. The corresponding values for Gr/Mg are 3% tensile modulus decrease for RT to 300°C (572°F) and 2% tensile strength variation for RT to 313°C (595°F). The large variation of tensile strength for Gr/Al was due to some failures in the grip areas which do not reflect the tensile strength of the material. It is believed that both the tensile and compressive modulus variations of Gr/Al and Gr/Mg material are small in the RT to 260°C (RT to 500°F) range. Thus, the 20% increase in the compressive modulus of Gr/Al from RT to 260°C (500°F) was surprising. More data are required to substantiate this observation.

During the test series, it was found that both the tensile and compressive moduli depend upon the thermal and loading history. Two Gr/Al specimens were heat treated to T6 condition for the aluminum matrix material and then were compressively tested at room temperature. A 33% compressive strength increase was observed for the heat treated specimens over the average compressive strength for the as-received condition. The higher strength was apparently due to a higher matrix contribution to the composite strength resulting from the heat treatment. The matrix heat treatment does not affect the tensile strength of Gr/Al to such an extent. Thus, it is postulated that the matrix strength properties have much more influence on the composite strength in compression than in tension. Two additional Gr/Al specimens, which were cooled to RT from a 260°C (500°F) preheating operation, had a measured tensile modulus of 2.32 and $2.42 \times 10^5 \text{ MN/m}^2$ (33.6 and 35.1 Msi) at RT, a 15 and 9% reduction, respectively, from the average RT tensile modulus without any preheating operation. The Gr/Al compressive specimen, which had similar cooldown to RT from 260°C (500°F) preheating, had a compressive modulus of $2.65 \times 10^5 \text{ MN/m}^2$ (38.5 Msi) following an RT tensile retest. This value is much higher than the average compressive modulus of nonpreheated specimens and is closer to the tensile modulus. It is postulated that the

residual stresses in the filament and the aluminum matrix, as a result of cooldown, change the mechanical characteristics of the composites. Further investigation is needed in this area.

B. ABSORPTANCE AND EMITTANCE TESTS

The results of the absorptance measurements as a function of temperature under CO_2 laser illumination ($10.6\ \mu m$) for all three samples are shown in Fig. 7. The absorptance for Gr/Al, Gr/Mg, and 6061-T6 Al between 200 and 500°C (392 and 932°F) remains constant at 0.06 to 0.08 with the exception that there is a dramatic increase in the absorptance of Gr/Mg (0.47) at 500°C (932°F). [When the calorimeter was disassembled, it was found that the carbon fibers were no longer embedded in magnesium, and the calorimeter surfaces closest to the sample were coated with a coarse silvery substance (see Fig. 8). This sublimation would explain the anomalous last point.]

The total hemispherical emittance measurements are shown in Fig. 9. The emittance for Gr/Mg is 0.2 at 200°C (392°F) and gradually decreases to about 0.17 at 400°C (752°F). As with the absorptance, there is a drastic change in the emittance (0.63) at 500°C (932°F). The emittance of 6061-T6 aluminum remains approximately constant between 200 and 350°C (392 and 662°F) at about 0.2. Between 300 and 500°C (572 and 932°F) there is a slight increase to about 0.22. The emittance for the Gr/Al agrees with that of the 6061 aluminum values at low temperature. At temperatures higher than 400°C (752°F), the emittance decreases. At 500°C (932°F) the emittance is 0.18.

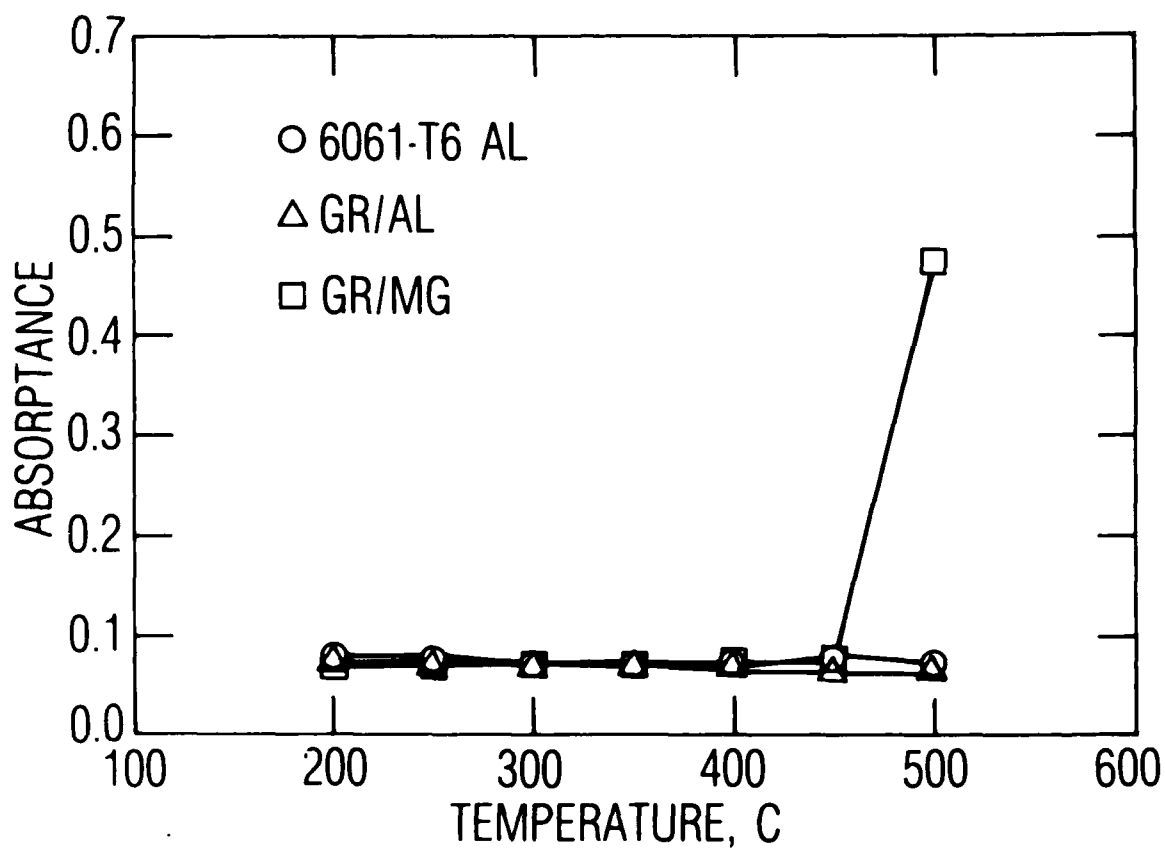


Fig. 7. Absorptance of 6061-T6 aluminum, graphite-aluminum, and graphite-magnesium as a function of temperature

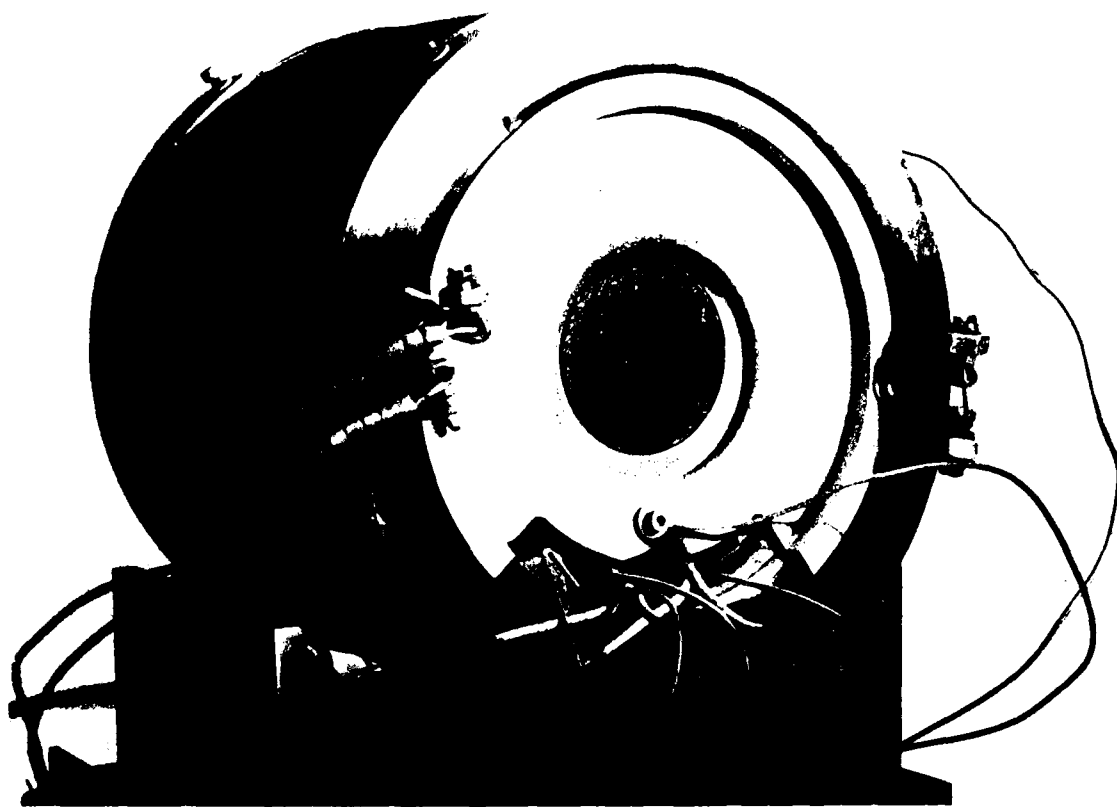


Fig. 8. Calorimeter disassembled after absorptance tests

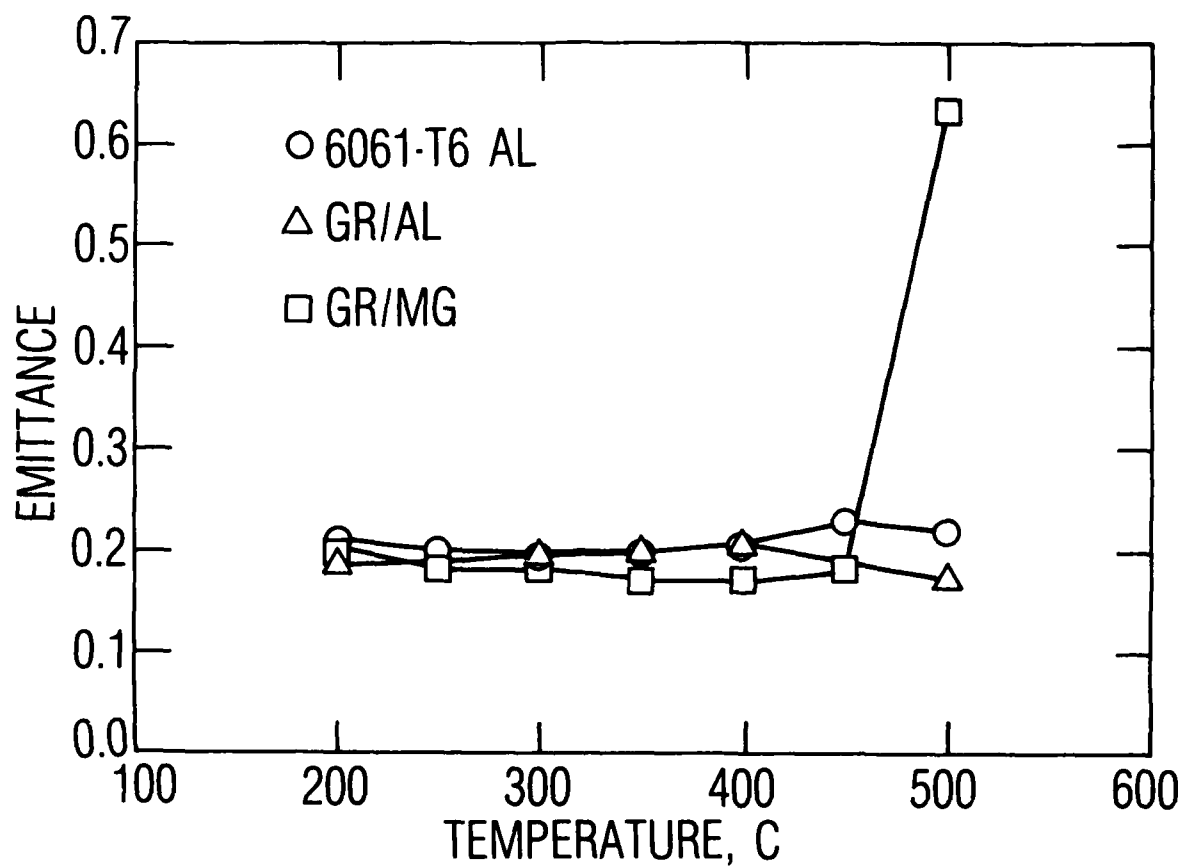


Fig. 9. Total hemispherical emittance of 6061 aluminum, graphite-aluminum, and graphite-magnesium as a function of temperature

V. CONCLUSIONS AND RECOMMENDATIONS

It can be seen from Tables 2 and 3 that the compressive modulus and strength values for Gr/Al and Gr/Mg differ from the tensile values. Room temperature compressive moduli for as-received Gr/Al and Gr/Mg materials are approximately 78 and 89%, respectively, of the tensile values. The corresponding room temperature compressive strength values are approximately 36% for Gr/Al and 58% for Gr/Mg of the tensile strength. There seems to have been a modulus increase from RT to both 149 and 260°C (300 and 500°F) for Gr/Al, whereas the modulus difference between 149 and 260°C (300 and 500°F) is negligible. For Gr/Mg material, the modulus difference for all temperatures up to 260°C (500°F) seems to be within the scatter band of the measurements.

The compressive strength values at 149°C (300°F) for Gr/Al and Gr/Mg are very close to the room temperature values. At 260°C (500°F), however, there is a significant drop in the compressive strength. The aluminum or magnesium matrices in either composite get much softer at 260°C (500°F). It is postulated that the softening of the matrix reduces the lateral support to the graphite fibers. Therefore, the fibers failed prematurely in buckling.

Note that the compressive data are too few in number to provide reliable design data. More tests must be performed to establish more accurate design data.

The values for the emittance and absorptance of Gr/Al, Gr/Mg, and 6061-T6 Al are very similar and appear reasonable. Even though small blisters were noticed when the Gr/Mg sample reached 300°C (572°F), they appeared on both samples, the one illuminated by the laser and the control sample. The small blisters cannot be attributed to laser damage, nor do they seem to have affected the overall experiment in any other way. Because of the low eutectic temperature of the constituents in AZ91C and AZ61A (such as zinc), the application of Gr/Mg at temperatures higher than 450°C is not recommended.

REFERENCES

1. Stuhrike, W. F., "The Mechanical Behavior of Aluminum-Boron Composite Material," Metal Matrix Composites, ASTM STP 438, 1958, pp. 108-133.
2. Metcalfe, A. G., "Fiber Reinforced Titanium Alloys," Composite Materials, Vol. 4, Chapter 6, edited by K. G. Kreider, Academic Press, N.Y., 1974.
3. "Structural Analysis Methods for Advanced Composites: 4. Structures and Materials," Report CASD-ERR-73-029, General Dynamics/Convair Aerospace Division, Dec. 1973.
4. "Design, Manufacture, Development, Test and Evaluation of Boron/Aluminum Structural Components for Space Shuttle, Vol. II - Materials and Processing," Report GDCA-DBG73-006, General Dynamics/Convair Aerospace Division, Aug. 1973.
5. "Development of Engineering Data on the Mechanical and Physical Properties of Advanced Composite Materials," AFML-TR-72-205, Part II, Contract No. F33615-71-C-1713, IIT Research Institute, Feb. 1974.
6. "Composite Box Beam Optimization: Experimental Data Supporting Technology Development and Preliminary Design," AFML-TR-73-13, Grumman Aerospace Corp., June 1973.
7. "Advanced Development of Conceptual Hardware - Fuselage," Report NA-73-662-8, Rockwell International/Los Angeles Aircraft Division, March 1974.
8. "Composite Box Beam Optimization, Vol II, Increased Structural Efficiency of Boron/Aluminum," AFML-TR-74-105, Grumman Aerospace Corp., May 1974.
9. "Boron/Aluminum Skins for the DC-10 Aft Pylon," NASA CR-132645, McDonnell Douglas Corp/Douglas Aircraft Co., May 1975.
10. "Manufacturing Methods for Metal Matrix Structural Components," Interim Report IR-304-4(W) for Contract F33615-74-C-5151, General Dynamics/Convair Division, 15 July 1975.
11. "Optimum Boron/Aluminum Design for a B-1 Wing Rib," NA-74-584-15, Contract 70-00626 (General Dynamics/Convair Division) Rockwell International/Los Angeles Aircraft Division, 1975.
12. "Boron/Aluminum Landing Gear for Navy Aircraft," Report CASD-NADC-76-003, General Dynamics, Convair Division, Sept. 1978.
13. Schromm, R. E., "Cryogenic Mechanical Properties of Boron, Graphite, and Glass Reinforced Composites," Materials Sciences and Engineering, 30(1977), 197-204.

14. E. G. Wolff, E. G. Kendall and W. C. Riley, "Thermal Expansion Measurements of Metal Matrix Composites," Advances in Composite Materials, A. R. Bunsell, Ed., ICCM III, Pavis, Pergamon Press, 1980.
15. H. H. Armstrong, A. M. Ellison, D. H. Kintis, P. G. Sullivan, "Development of Graphite/Metal Advanced Composites for Spacecraft Applications," IMSC-D758140, 15 April 1980.
16. R. E. Taylor and H. Groot, "Thermophysical Properties of Fiber-Reinforced 6061," PRL524, Properties Research Laboratory, West Lafayette, Indiana, May 1980.
17. R. E. Taylor and H. Groot, "Thermophysical Properties of Graphite Aluminum and Graphite Magnesium," PRL 330, Properties Research Laboratory, West Lafayette, Indiana, June 1984.
18. Adsit, N. R., "Compression Testing of Graphite/Epoxy," Compression Testing of Homogeneous Materials and Composites, ASTM STP 808, Richard Chait and Ralph Papirno, eds., ASTM, 1983, pp. 175-186.
19. F. Izaguirre, L. Fishman, "A Calorimetric Approach for Measuring Emittance and Normal Spectral Absorptance at Elevated Temperatures," in AIAA 19th Thermophysics Conference, Snowmass, CO, 25-28 June 1984.

LABORATORY OPERATIONS

The Aerospace Corporation functions as an "architect-engineer" for national security projects, specializing in advanced military space systems. Providing research support, the corporation's Laboratory Operations conducts experimental and theoretical investigations that focus on the application of scientific and technical advances to such systems. Vital to the success of these investigations is the technical staff's wide-ranging expertise and its ability to stay current with new developments. This expertise is enhanced by a research program aimed at dealing with the many problems associated with rapidly evolving space systems. Contributing their capabilities to the research effort are these individual laboratories:

Aerophysics Laboratory: Launch vehicle and reentry fluid mechanics, heat transfer and flight dynamics; chemical and electric propulsion, propellant chemistry, chemical dynamics, environmental chemistry, trace detection; spacecraft structural mechanics, contamination, thermal and structural control; high temperature thermomechanics, gas kinetics and radiation; cw and pulsed chemical and excimer laser development including chemical kinetics, spectroscopy, optical resonators, beam control, atmospheric propagation, laser effects and countermeasures.

Chemistry and Physics Laboratory: Atmospheric chemical reactions, atmospheric optics, light scattering, state-specific chemical reactions and radiative signatures of missile plumes, sensor out-of-field-of-view rejection, applied laser spectroscopy, laser chemistry, laser optoelectronics, solar cell physics, battery electrochemistry, space vacuum and radiation effects on materials, lubrication and surface phenomena, thermionic emission, photo-sensitive materials and detectors, atomic frequency standards, and environmental chemistry.

Computer Science Laboratory: Program verification, program translation, performance-sensitive system design, distributed architectures for spaceborne computers, fault-tolerant computer systems, artificial intelligence, micro-electronics applications, communication protocols, and computer security.

Electronics Research Laboratory: Microelectronics, solid-state device physics, compound semiconductors, radiation hardening; electro-optics, quantum electronics, solid-state lasers, optical propagation and communications; microwave semiconductor devices, microwave/millimeter wave measurements, diagnostics and radiometry, microwave/millimeter wave thermionic devices; atomic time and frequency standards; antennas, rf systems, electromagnetic propagation phenomena, space communication systems.

Materials Sciences Laboratory: Development of new materials: metals, alloys, ceramics, polymers and their composites, and new forms of carbon; non-destructive evaluation, component failure analysis and reliability; fracture mechanics and stress corrosion; analysis and evaluation of materials at cryogenic and elevated temperatures as well as in space and enemy-induced environments.

Space Sciences Laboratory: Magnetospheric, auroral and cosmic ray physics, wave-particle interactions, magnetospheric plasma waves; atmospheric and ionospheric physics, density and composition of the upper atmosphere, remote sensing using atmospheric radiation; solar physics, infrared astronomy, infrared signature analysis; effects of solar activity, magnetic storms and nuclear explosions on the earth's atmosphere, ionosphere and magnetosphere; effects of electromagnetic and particulate radiations on space systems; space instrumentation.

END

2-87

DTIC